XXXVI Ibero-Latin American Congress on Computational Methods in Engineering

CILAMCE

Rio de Janeiro, 22-25 Nov 2015

A MULTI-OBJECTIVE OPTIMIZATION OF A SOLAR SAILCRAFT TRAJECTORY IN AN EARTH-MARS TRANSFER USING AN EVOLUTIONARY ALGORITHM

Igor Mainenti-Lopes

Luiz Carlos Gadelha de Souza

Fabiano Luis de Sousa

iml.lopes@pq.cnpq.br

lcgadelha@gmail.com

fabiano.sousa@inpe.br

Instituto Nacional de Pesquisas Espaciais

Av. dos Astronautas, 1.758, Jd. da Granja, 12227-010, São José dos Campos-SP, Brazil

Abstract. *The goal of this work was a multi-objective analysis of a solar sailcraft trajectory optimization in an Earth-Mars transfer. Solar sailcraft is a propulsion system with great interest in space engineering, since it uses solar radiation to propulsion. So there is no need for propellant to be used, thus it can remains active throughout the entire transfer maneuver. This type of propulsion system opens the possibility to reduce the cost of exploration missions in the solar system. In its simplest configuration, a Flat Solar Sail (FSS) consists of a large and thin structure generally composed by a film fixed to flexible rods. The performance of these vehicles depends largely on the sails attitude relative to the Sun. Using a FSS as propulsion, an Earth-Mars transfer optimization problem was tackled by the M-GEO*$_{real}$ *algorithm (Multi-objective Generalized Extremal Optimization with real codification). This algorithm is an Evolutionary Algorithm (AE) based on the theory of Self-Organized Criticality. The FSS was able to perform up to 20 maneuvers until reach the Mars orbit. The M-GEO*$_{real}$ *had the task to optimize 21 variables (20 attitude angles e the time between maneuvers) that minimize the transfer time to reach the Mars orbit and the total number of maneuvers necessary to achieve that goal. The M-GEO*$_{real}$ *algorithm succeeded to return an optimize frontier for this problem with 5 non-dominated solutions. However, a second attempt to achieve an optimize frontier shown better performance. It consisted in run a SQP algorithm (Sequential Quadratic Programming) with the M-GEO*$_{real}$ *solutions as initial guesses. As result 4 better non-dominated solutions were reached and one of M-GEO*$_{real}$ *solution becomes dominated by the new solutions.*

Keywords: *Solar Sailcraft, Trajectory Optimization, Multi-Objetictive Problem, Evolutionary Algorithm, Generalized Extremal Optimization*

INTRODUCTION

The design and optimization of interplanetary transfer trajectory is one of the most important tasks during the design phase of an exploration mission due to the large increases of speed needed for the transfer. Low-thrust propulsion systems can improve significantly or even becomes feasible missions (Dachwald, 2004). One of these kinds of propulsion system is the solar sailcrafts. The solar sailcraft need to be a large, thin and flexible structure so that it can generate the maximum thrust with the minimum weight. Generally, the films are clamped at thin beams. In other hand, the film needs to be resistant enough to handle with attitude maneuvers. Its function is to use the pressure of solar radiation to generate thrust on the vehicle. The performance of the FSS depends mainly on its attitude. Its control presents great difficulties because the effects of structural vibration caused by its high flexibility. Moreover, obtaining optimal trajectories using low propulsion can become a job that requires excessive time work involving a lot of experience and expert knowledge in control theory and orbital mechanics (Dachwald, 2004). In this sense, it is interesting to seek efficient ways to tackle this type of optimization problem.

A method that has shown good performance by tackling complex optimization problems in engineering and science are Evolutionary Algorithms (EA) (Clarck *et al*., 2000, Dasgupta and Michalewicz, 2001 and Eiben and Smith, 2003). De Sousa et al. (2003) developed an AE called Generalized Extremal Optimization (GEO - Generalized Extremal Optimization). It is easy to implement, it does not use derivatives and it can be used in problems with or without constraints. The design space can presents non-convex or even disjoint regions. This algorithm is able to handle problems with any combination of continuous variables, discrete or integer. Several versions of the GEO have been developed, including hybrid and multi-objective versions (Galski 2006), and it has proved to be very competitive when tackling test functions and design optimization problems.

Considering the characteristics presented by the GEO algorithm, a multi-objetive version of GEO able to work directly with real variables, called M-GEO$_{real}$, is a promising method to achieve good results for the problem proposed (Mainenti-Lopes, 2013). In this work, the M-GEO$_{real}$ was used to optimize two different objective functions simultaneously: the transfer time between Earth and Mars orbits and the total numbers of maneuvers to accomplish this goal. The following simplifications were considered: the Earth and Mars orbits were considered circular, concentric and coplanar. The maximum number of 20 attitude maneuvers to be performed by the FSS during transfer was imposed and the time that the FSS stay at each attitude angle was the same. Therefore, the algorithms were used to optimize 21 variables: 20 attitude angle and 1 time value. Besides, the forces acting on the sail are only the forces from Sun gravitational field and from solar radiation pressure generated by the FSS itself. It was assumed that all the mass of the Sun is concentrated at one point and it is a point light source.

The M-GEO$_{real}$ returned 5 optimized solutions for this problem. However, 3 of those solutions were dominated by a result obtained by GEO$_{real1}$, a mono-objeticve version of GEO algorithm, presented in Mainenti-Lopes et al. (2014) work.

With the intent to improve the solutions obtained by M-GEO$_{real}$, they were used as initial guesses using a Sequential Quadratic Programming algorithm (SQP). Only the transfer time was optimized by SQP algorithm. As result, 4 better solutions were obtained and one solution does not present improvements, so it becomes dominated by the others.

1 METHODOLOGY

1.1 Mathematical model of the Flat Solar Sailcraft

In this work, the mathematical formulation of a Flat Solar Sailcraft (FSS) obtained from Zhang et al. (2010) work was considered. In this mathematical formulation will not be considered disturbance torques during the transfer trajectory. However, it is assumed that the sail film have a non-specular reflection. Furthermore, this study was considered a transfer between circular orbits in the same plane. Using cylindrical coordinates, the state vector is given by

$$x_e = \begin{bmatrix} r \\ \theta \\ u \\ v \end{bmatrix} \tag{1}$$

where r is the distance between the FSS and the Sun, θ is the polar angle, u and v are the radial and tangential velocities of the FSS, respectively. In Figure 1 a graphical representation of the position of the solar sail related with the sun and the state variables is presented.

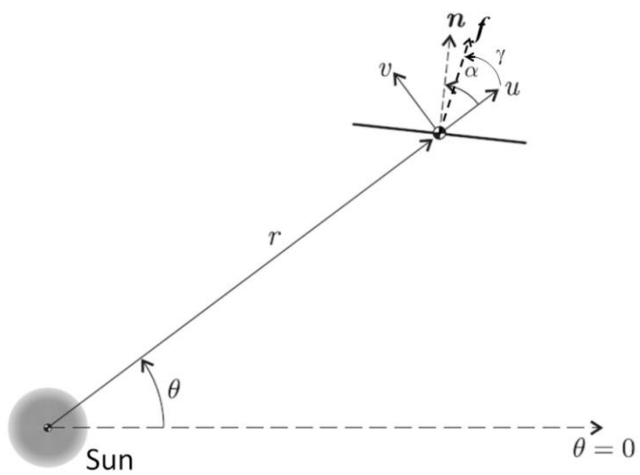

Figure 1. A graphical representation of the state variables. f is the unit vector in the direction of the radiation pressure force and γ is the angle between a f and r̂.

Considering the coordinates presented in Eq. (1), the equations of motion can be written as

$$\dot{x}_e = \begin{bmatrix} u \\ v/r \\ \frac{v^2}{r} - \frac{GM}{r^2} \\ -uv/r \end{bmatrix} + \begin{bmatrix} 0 \\ 0 \\ b_1 + b_2\cos^2\alpha + b_3\cos\alpha \\ \sin\alpha\,(b_2\cos\alpha + b_3) \end{bmatrix} . a_c \left(\frac{r_o}{r}\right)^2 \cos\alpha \tag{2}$$

The Eq. (2) first term represents the solar gravitational acceleration and the second term the FSS acceleration. G is the universal gravitational constant, M is the mass of the Sun, $r_o = 1$ UA, $\alpha \in [-\pi/2, \pi/2]$ is the FSS attitude angle, a_c is the characteristic acceleration and b_1, b_2 and b_3 are FSS film optical parameters. The full deduction of these FSS equations of motions is presented in Mainenti-Lopes et al. (2014) work.

1.2 Units Convention for the Proposed Problem

In studies of interplanetary trajectories and transfers problems a specific set of units is widely used. Those units are: astronomical unit (AU) to distance and radians (rad) for time. The transformation of meters (m) to AU is trivial: $1\ \mathrm{AU} = 1.4959787 \times 10^{11}$ m. The unit transformed of time variable is according with Earth orbital motion. It is known that the Earth takes one year for turn around the sun and it represents a rotation of 2π rad. Therefore, it can be write as $1\ \text{year} = 2\pi$ rad. This relation in seconds is $1\ \mathrm{s} = 1{,}99096677 \times 10^{-7}$ rad.

The main advantage of this unit transformation is to ensure that the values of distance and time will never be too big or too small over the entire numerical integration process. Thus, this strategy allows to avoid computational problems with numerical representation. Thus, the constant evolved in Equation 8 can be written using the following units:

- $\mathrm{unit[GM]} = \mathrm{AU^3/rad^2}$;
- $\mathrm{unit}[\mathrm{a_c}] = \mathrm{AU/rad^2}$.

Using the proposed units, it can be verified that $\mathrm{GM} = 1{,}0\ \mathrm{UA^3/rad^2}$ and considering the characteristic acceleration value equal to $1{,}0\ \mathrm{mm/s^2}$, then $\mathrm{a_c} = 0{,}16863441\ \mathrm{UA/rad^2}$.

1.3 Optimization Algorithms

1.3.1 M-GEO$_{\text{real}}$ Algorithm

Multi-objective optimizations problems consist in optimize simultaneously two or more conflicting objectives. Because the objectives are conflicting, it is impossible to obtain one solution that optimizes all objectives. Therefore, one can obtain a set of solutions that, for each solution, it is impossible to optimize one objective without losing optimality in the others. This set of solution in the design space is called Pareto Set and in the objective space is called Pareto Front. The main goal of an algorithm capable to tackle multi-objective problems is to obtain Pareto Set and Pareto Front.

M-GEO$_{\text{real}}$ was based on an algorithm presented by Mainenti-Lopes et al. (2008), called GEO$_{\text{real}}$. The main difference between GEO$_{\text{real}}$ and M-GEO$_{\text{real}}$ is how each one deals with the best solution. As a mono-objective algorithm, GEO$_{\text{real}}$ stores the best solution along the run and returns only one solution. While M-GEO$_{\text{real}}$ stores the non-dominated solutions along the run and for each new solution a test is made to determine which solution will be kept and which will be discarded. The following steps give this test that will be called Pareto Front Test in this work:

(i) test if the new solution is dominated by any solution in the stored Pareto Front. That is, if any solution in Pareto Front is at least equal in all objective functions except for one that is better than the new solution. If the new solution is dominated, keep the Pareto Front and go to the step (iii). Otherwise, include the new solution and go to the next step;

(ii) determine all solutions that the new solution dominate and discard them from the Pareto Front;

(iii) finish the Pareto Front Test.

M-GEO$_{\text{real}}$ was developed to recover the Pareto Front and the Pareto Set maintaining the main characteristic of GEO algorithm. The flowchart of M-GEO$_{\text{real}}$ is presented in Fig. 2.

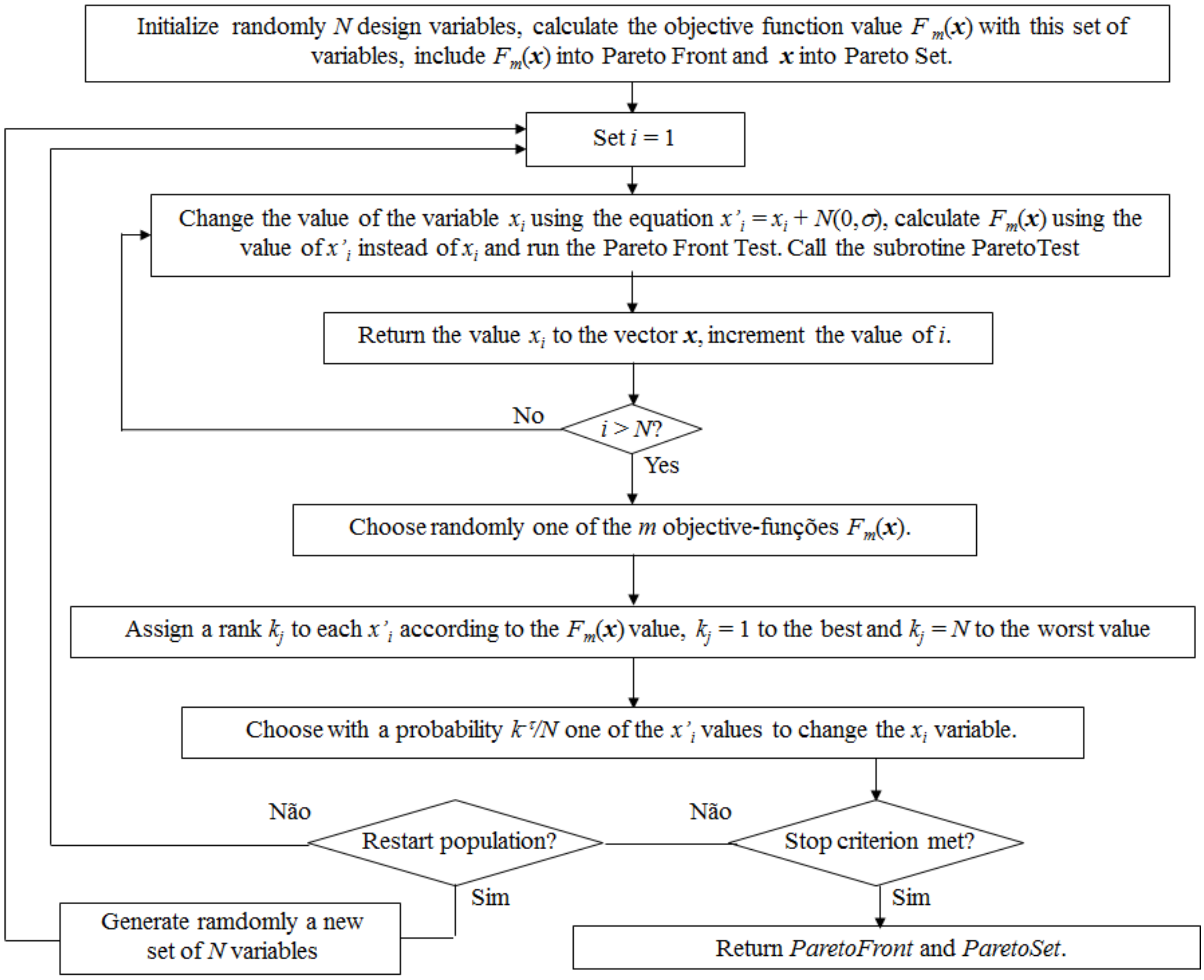

Figure 2. M-GEOreal flowchart.

The population restart test is made to increase the algorithm capacity to recover all Pareto Front. In this work, the criterion to restart the population was given by the free parameter rt that represents the number of restarts along the search.

1.3.2 SQP Algorithm

The Sequential Quadratic Programming algorithm is able to tackle nonlinear optimization problems described by

$$\mathcal{F} = \begin{cases} \min_{x \in \mathbb{R}^n} f(x) \\ l \leq x \leq u \\ c_I(x) \leq 0 \\ c_E(x) = 0 \end{cases} \tag{3}$$

where $f: \mathbb{R}^n \to \mathbb{R}$, $c_I: \mathbb{R}^n \to \mathbb{R}^{m_I}$ and $c_E: \mathbb{R}^n \to \mathbb{R}^{m_E}$ are smooth nonlinear functions that can be non-convex. $c_I(x)$ and $c_E(x)$ are the equality and inequality constraints functions, respectively. The inequality $l \leq \left(x, c_I(x)\right) \leq u$ represents the boundary constraints of x and

$c_I(x)$. The lower and upper constraints l and $u \in \mathbb{R}^{n+m_I}$ must satisfy $l < u$. Moreover, the problem $\mathcal{F}$ has $m_I \geq 0$ nonlinear constraints of inequality and $m_E \geq 0$ of equality.

The solution of the problem $\mathcal{F}$ is a vector $\vec{x}^*$ of n components that satisfies all constraints of $\mathcal{F}$. Moreover, $f(\vec{x}^*)$ must be a better value than any other feasible $f(\vec{x})$.

The optimality conditions for a local minimum of the problem $\mathcal{F}$ are given by the Karush-Kuhn-Tucker (KKT) conditions (Zhang et al. 2010). At the local minimum, $(\vec{x}, \lambda, \mu)$ satisfies

$$\nabla J(\vec{x}) - \sum_{i=1}^{m_E} \lambda_i \nabla c_{Ei}(\vec{x}) - \sum_{j=1}^{m_I} \mu_j \nabla c_{Ij}(\vec{x}) = 0; \tag{4}$$

$$c_{Ei}(\vec{x}) = 0, i = 1, \ldots, m_E; \tag{5}$$

$$c_{Ij}(\vec{x}) \geq 0, \mu_j \geq 0, \mu_j \nabla c_{Ij}(\vec{x}) = 0, j = 1, \ldots, m_I \tag{6}$$

where the notation ∇ represents the gradient with respect to $\vec{x}$, $\lambda^T = (\lambda_1, \ldots, \lambda_{m_1})$ and $\mu^T = (\mu_1, \ldots, \mu_{m_2})$.

The KKT conditions are the necessary first order conditions for a optimal solution in nonlinear programming. The KKT approach generalizes the method of Lagrange multiplier, by allowing the inclusion of inequality constraints. The system of equations corresponding to the KKT conditions is generally not solved directly, except in a few special cases where solutions can be derived analytically. In general, many optimization algorithms can be employed as methods to numerically solve the system of KKT equations (Boyd & Vandenberghe 2004).

1.4 Application of the algorithm to the optimization problem

The trajectory optimization of a FSS is obtained by defining its attitude with respect to time. That´s mean, $\alpha^*(t)$ should be found, where $\alpha(t)$ is the function that describes the FSS attitude history. In general, this function can take any form as long as its image remain confined between $-\pi/2$ and $\pi/2$, which are the possible values for the FSS attitude angle in normal operation. An example of how this function can behave is presented graphically in Figure 3 (solid line).

The approach adopted in this work considers that the function $\alpha(t)$ is transformed in a sum of several step functions, as shown in Figure 3 (dashed line). Thus, to determine the function, it is necessary to define a set of values of the steps and the time spent in each step. This strategy can be interpreted that $\alpha(t)$ function was discretized and can be characterized by the vectors $\vec{\alpha}$ and $\vec{T}_{int}$, which are, respectively, the vectors of the FSS attitude angles and time that it remains in each steps. Therefore, the number of elements N_m of these two vectors must be equal and represents the maximum number of maneuvers performed by the FSS during the transfer.

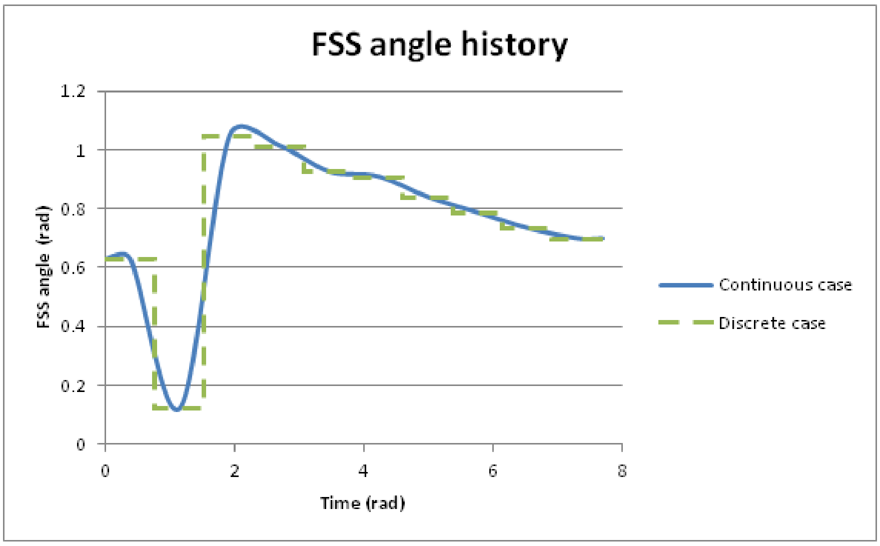

Figure 3. Graphical representation of the FSS angle history relative to the Sun, for the continuous case (solid line) and discrete case (dashed line).

The optimization problem tackled in this work can be characterized as follows:

$$\begin{cases} \mathrm{Min}\ F_1 = k_1.T_{rend} + k_2.\left(r_M - r(T_{rend})\right)^2 + k_3.\left(u(T_{rend})\right)^2 + k_4.\left(v_M - v(T_{rend})\right)^2 \\ \mathrm{Min}\ F_2 = N_{maneuver} \end{cases} \quad (7)$$

Subject to the restrictions

$$\begin{cases} -\pi/2 \le \alpha_j \le \pi/2 \\ 0{,}057\mathrm{rad} \le T_m(j) \le 0{,}12\mathrm{rad} \end{cases} \quad (8)$$

with $j = 1, 2, 3, \dots, 20$

and the dynamics of solar sail given by

$$\dot{\vec{x}}_e = \begin{bmatrix} u \\ v/r \\ \frac{v^2}{r} - \frac{GM}{r^2} + (b_1 + b_2\cos^2\alpha + b_3\cos\alpha).\epsilon \\ -\frac{uv}{r} + \sin\alpha\,(b_2\cos\alpha + b_3).\epsilon \end{bmatrix} \quad (9)$$

where $\epsilon = a_c(r_o/r)^2\cos\alpha$, F_1 is the objective function which is the sum of the FSS transfer time and the rendezvous error with the Mars orbit. The function F_1 was obtained from the work of Zhang et al. (2010), where k_1, k_2, k_3 and k_4 are weights, T_{rend} is the rendezvous instant, r_M is the semi-major axis of the Mars orbit, $r(T_{rend})$ is the FSS distance from the Sun in the integration instant T_{rend} and $u(T_{rend})$ and $v(T_{rend})$ are, respectively, radial and tangential components of the FSS velocity. In the case where the FSS do not rendezvous the Mars orbit, T_{rend} assumes the value of $20 \times \max(T_m)$ which is the maximum integration time. F_2 is the total numbers of maneuvers that the FSS execute to reach Mars orbit.

The values used as weights in F_1 function were obtained from the work of Zhang et al. (2010), processed according to the units convention adopted in Section 1.2 and normalized to $k_1 = 1$. Thus, $k_2 = 1{,}4 \times 10^6$, $k_3 = 7{,}5 \times 10^6$ and $k_4 = 3{,}0 \times 10^6$. Table 1 shows the values considered for entry into Mars orbit.

Table 1. Mars orbit states and the errors associated with them.

Simbol	Parameters names	Value	Units
r_M	Mars orbit semi-major	1,523	AU
u_M	Mars orbit radial velocity	0	AU/rad
v_M	Mars orbit tangential velocity	0,810	-
e_r	associated error of r component	0,002	AU
e_u	associated error of u component	0,002	AU/rad
e_v	associated error of v component	0,002	-

2 RESULTS

In this section the results for the multi-objective approach of a FSS trajectory optimization is presented and described. Initial tests were run in order to define the M-GEO$_{real}$ free parameters values. The following methodology was used to define those free parameters:

1. Define arbitrarily values for all free parameters except for the τ parameter. The initial values of the parameters were fixed to $\sigma = 50\%$ of the variable range and $\mathrm{rt} = 20$.
2. It was performed a run with 5×10^5 evaluations of the objective function for each τ values tested. The values of τ tested were $\{1,2,3, \dots ,8\}$.
3. From the optimized frontier obtained in step 2, it was chosen the best τ value.
4. The τ value was set according to previously choice and the same process done with τ parameter was proceed to choose the σ parameter.
5. The values of σ tested were $\{10\%, 20\%, 30\%, \dots , 100\%\}$.
6. From the optimized frontier obtained in step 5, it was chosen the best σ value.
7. Finally, the rt value was chosen using the same procedure presented for τ and σ choice. The values of σ tested were $\{10, 20, 30,40, 50\}$.

After performing the above procedure the following parameters values had been defined GEO$_{real1}$: $\tau = 2$, $\sigma = 50\%$ and $\mathrm{rt} = 20$.

In Figure 4 is presented the optimized frontier for the problem proposed in this work. The blue diamonds are solution obtained using M-GEO$_{real}$. The red square was obtained by Mainenti-Lopes *et al*. (2014) using a mono-objective version of M-GEO$_{real}$. The Mainenti-Lopes *et al*. (2014) solution dominated 3 solution obtained in this work. It indicates that M-GEO$_{real}$ could find better solutions.

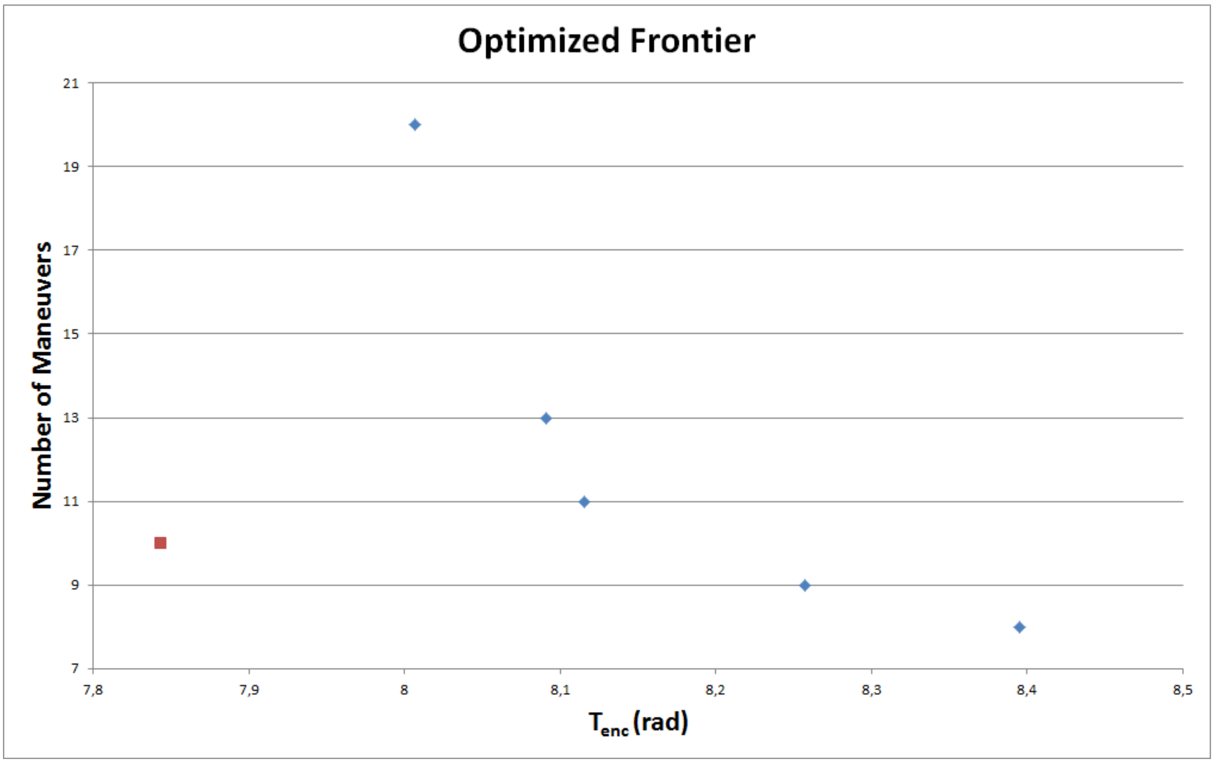

Figure 4. Optimized frontier of the multi-objective problem of FSS trajectory. The blue diamonds are solution obtained using M-GEO$_{real}$ and the red square was obtained by Mainenti-Lopes (2014).

In Figure 5, the FSS attitude angle versus time of the lower and the higher values of maneuvers obtained are presented.

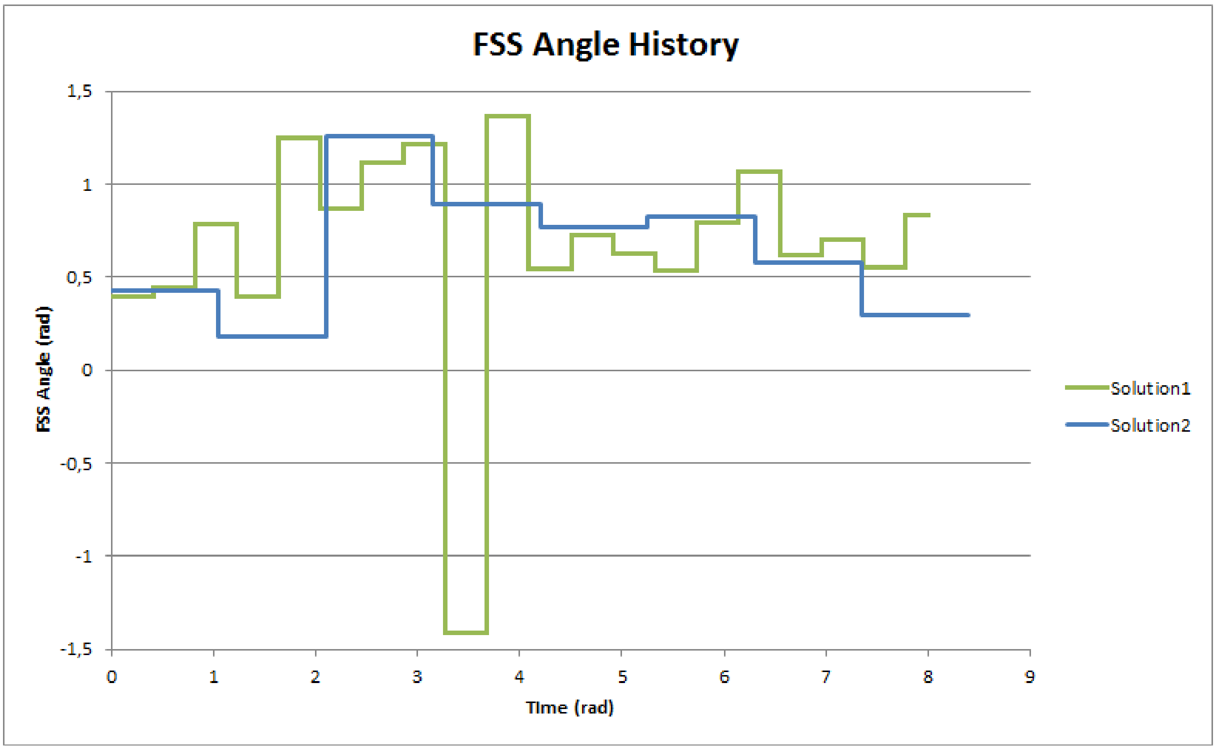

Figure 5. FSS attitude angle versus time of the best solution with 8 maneuvers (blue line). b. Trajectory of the best solution with 20 maneuvers (green line).

The FSS trajectories of the lower and the higher values of maneuvers obtained are presented in Figure 6.

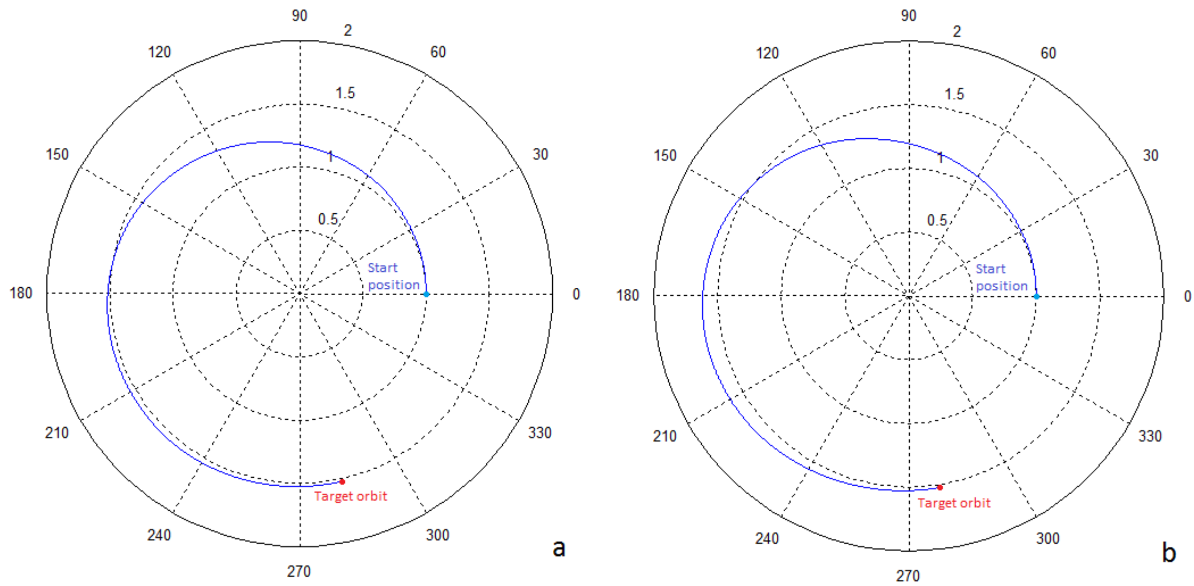

Figure 6. a. Trajectory of the best solution with 8 maneuvers. b. Trajectory of the best solution with 20 maneuvers.

In order to improve the result obtained by M-GEO$_{real}$ the SQP algorithm was used. Each of 5 solutions presented in Figure 4 was used as initial guesses for SQP runs. The SQP was implemented so that it could optimize only the transfer time, keeping the number of maneuvers unchanged. Table 2 presents a comparison between the solutions using only M-GEO$_{real}$ and using SQP algorithm too.

Table 2 – Comparison between results obtained using only M-GEO$_{real}$ with results obtained using SQP to optimize the M-GEO$_{real}$ results.

Solution	T_{enc} (rad): M-GEO$_{real1}$	Number of Maneuvers	T_{enc} (rad): SQP
1	8,0067	20	-
2	8,0913	13	7,8384
3	8,1158	11	7,9471
4	8,2574	9	8,2453
5	8,3953	8	8,3703

As result, 4 better solutions were obtained. The solution number 1 didn't present improvements so it become dominated by the others solutions. The new optimized frontier is presented in Figure 7.

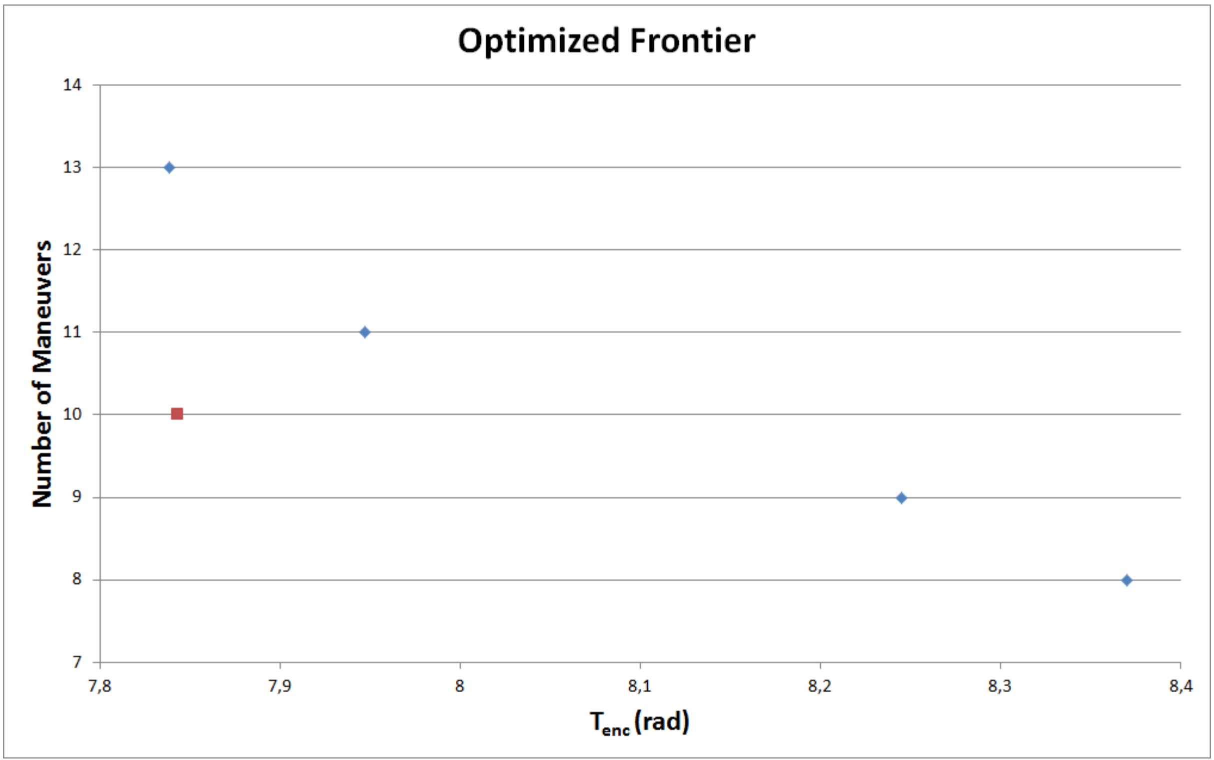

Figure 7. Optimized frontier of the multi-objective problem of FSS trajectory. The blue diamonds are solution obtained using M-GEO$_{real}$ + SQP and the red square was obtained by Mainenti-Lopes (2014).

3 CONCLUSIONS

In this paper a multi-objective problem of a FSS trajectory optimization was proposed. In the approach presented, it was considered transfers between circular, coplanar and centered on the Sun orbits. The starting orbit has radius equal to the semi-major axis of the Earth orbit and the target orbit radius is equal to the semi-major axis of the Mars orbit. The M-GEO$_{real}$ algorithm was used to optimize simultaneously the FSS transfer time and the number of maneuver to fulfill this task.

As result preliminaries results, 5 optimized solutions were obtained. However, 3 of those solutions were dominated by a solution obtained in the specialized literature, which it indicates that the M-GEO$_{real}$ solutions could become better. Therefore, the 5 M-GEO$_{real}$ solutions were used as initial guesses for a SPQ algorithm in an attempt to improve them. The attempt shown good result improving 4 of 5 solutions and it returned a better optimized frontier. This procedure indicates that a hybrid version of M-GEO$_{real}$ with a deterministic algorithm could present good results for this kind of optimization problem.

ACKNOWLEDGEMENTS

This research was developed with a CNPq -Brazil scholarship.

REFERENCES

Clarck, D.E, Mannhold, R., Kubinyi, H. & Timmerman, H. Evolutionary algorithms in molecular design. Weinheim: Whiley-VCH, 2000.

Dachwald, B. Low-Thrust Trajectory Optimization and Interplanetary Mission Analysis Using Evolutionary Neurocontrol. Doctor Tesis - Universität der Bundeswehr München Fakultät für Luft- und Raumfahrttechnik Institut für Raumfahrttechnik, 2004.

Dasgupta, D. & Michalewicz, Z. (Editores), Evolutionary Algorithms in: Engineering applications. Berlin, Heidelberg, New York: Springer, 2001.

De Sousa, F.L., Ramos, F.M., Paglione, P. & Girardi, R.M. New Stochastic Algorithm for Design Optimization, AIAA journal, Vol. 41, Number 9, pp. 1808-1818, 2003 (ISNN 0001-1452).

Eiben, A. E. & Smith, J.E. Introduction to evolutionary computing. Berlin: Springer, 2003.

Galski, R. L. Desenvolvimento de versões aprimoradas híbridas, paralela e multiobjetivo do método da otimização extrema generalizada e sua aplicação no projeto de sistemas espaciais. 2006-09-22. 279 p. (INPE-14795-TDI/1238). Doctor Tesis - Instituto Nacional de Pesquisas Espaciais, São José dos Campos. 2006.

Mainenti-Lopes, I., 2008, “Satellite Attitude Control of Rigid-Flexible Satellite Using the Generalized Extremal Optimization with a Multi-Objective Approach (in portuguese)”, Master Thesis, Nacional Institute for Space Research (INPE).

Mainenti-Lopes, I. 2013. An approach for multi-objective op-timization solar sail trajectories. Doctor thesis (in portuguese), INPE, São José dos Campos.

Mainenti-Lopes, I., Souza, L . C . G ., De Sousa F . L . Application of Generalized Extremal Optimization (GEO) Technique to Design the Orbit Transfer Solar Sail Control System. Engineering Optimization 2014. CRC Press 2014. Pages 219–224. Print ISBN: 978-1-138-02725-1. eBook ISBN: 978-1-315-73210-7. DOI: 10.1201/b17488-41.

Zhang, M., Wang. G. & Sun, Y. Solar Sail Trajectory Optimization for Earth-Mars Mission Proceedings of the 29th Chinese Control Conference. July 29-31, 2010, Beijing, China